Miralem HADŽISELIMOVIĆ[1,2], Viktor GORIČAN[2], Tine MARČIČ[3], Peter VIRTIČ[1,2], Bojan ŠTUMBERGER[1,2]

University of Maribor, Faculty of Energy Technology (1)
University of Maribor, Faculty of Electrical Engineering and Computer Science (2)
TECES, Research and Development Centre for Electric Machines (3)

Magnetic field analysis in slotless PM linear motor model: comparison of calculated and measured results

Abstract. *The article presents a magnetic field analysis in slotless permanent magnet linear motor model. The two types of magnetic field calculation are presented. The first one is analytical calculation of magnetic field in Polar coordinate system considering the linear motor model geometry. The second one is numerical calculation based on finite element method. In both calculations the normal and tangential components of the magnetic flux density in the air-gap are calculated. In order to make adequate analysis of magnetic field and to confirm calculation results the experimental setup for magnetic field measurement in slotless permanent magnet linear motor model was developed. Comparison of calculated and measured results is presented in paper as well.*

Streszczenie. *W artykule przedstawiono analizę pola magnetycznego w modelu bezżłobkowego silnika liniowego z magnesem trwałym. Dwa sposoby obliczania pola magnetycznego są prezentowane: obliczenia analityczne pola magnetycznego w biegunowym układzie współrzędnych, uwzględniającym geometrię modelu i obliczenia numeryczne oparte na metodzie elementów skończonych. W obu metodach obliczeniowych wyznacza się składowe normalne i styczne indukcji magnetycznej w szczelinie powietrznej. W celu weryfikacji adekwatności modelu i weryfikacji obliczeń wykonany został zestaw eksperymentalny dla pomiarów pola magnetycznego. Przedstawiono zostało porównanie wyników obliczeń i pomiarów. (**Analiza pola magnetycznego w modelu bezżłobkowego silnika liniowego z magnesem trwałym**)*

Keywords: magnetic field, permanent magnets, analysis, calculation, measurement.
Słowa kluczowe: pole magnetyczne, magnesy trwałe, analiza, obliczenia, pomiar

Introduction

In the process of designing the permanent magnet synchronous motors two different types of magnetic field calculations are usually used. The first type of calculation is analytical calculation of magnetic field quantities in the motor's air-gap and yoke (solution of magnetic field distribution is obtained in the explicit form). The second type of calculation is calculation of magnetic field distribution in the machine by using numerical methods, usually based on the finite element method. Analytical calculation is in comparison with the numerical calculation significantly faster, which means that the computational time is smaller with the same properties of used hardware in personal computer. On the other hand, the calculation of magnetic field distribution inside the all parts of motor is more precise by using numerical methods. Normally for the designing of permanent magnets motors both aforementioned approaches are used separately or simultaneously.

Several authors use in their research works analytical [1-5] or numerical calculations of magnetic field distribution for confirmation of theirs developed models. Results of calculations are only rarely confirmed with the experimental results. The main idea of this paper is to present comparison of calculated and measured results of magnetic field distribution in the air-gap of simple slotless permanent magnet linear motor model. Experimental setup for the measurement of magnetic field distribution in the air-gap of slotless permanent magnet linear motor model is presented in order to verify accuracy of the presented calculated results.

Table 1. Properties of used permanent magnets

B_r (T)	H_{cB} (kA/m)	H_{cJ} (kA/m)	$(BH)_{max}$ (kJ/m^3)	T_{max} (°C)
1,22-1,25	≥ 907	≥ 1592	287-310	150

Presentation of Slotless PM Linear Motor Model

The slotless permanent magnet linear motor model is build from two iron plates and two permanent magnets (Fig. 1). Iron plate size: length 364 mm, width 80 mm and thickness 10 mm. Permanent magnet size: length 86 mm, width 32 mm and thickness 2 mm. Distance between the iron plates is 7,75 mm and the air-gap thickness is 5,75 mm. In such a way composed two pole slotless permanent magnet linear motor model is shown in Fig. 2. Properties of used neodymium permanent magnets (NdFeB) are presented in Table. 1.

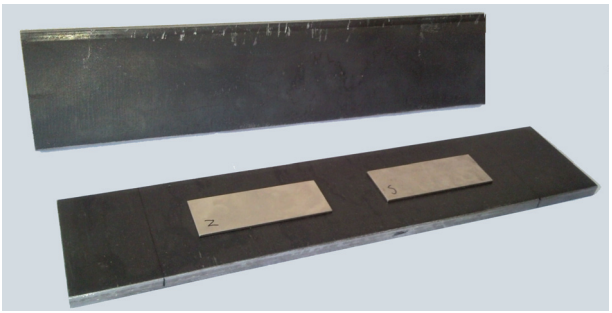

Fig.1. Parts of slotless permanent magnet linear motor model.

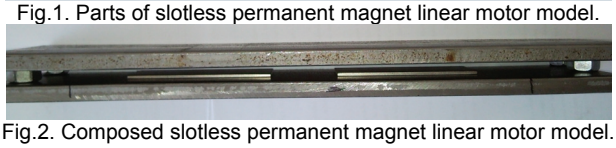

Fig.2. Composed slotless permanent magnet linear motor model.

Analytical solution of magnetic field distribution in the air-gap

In the presented slotless PM linear motor model with two iron plates and two magnets, the empty space below the first iron plate represents the place for slotless iron core and the second iron plate carry surface mounted permanent magnets. Analytical solution of magnetic field distribution in the PM linear motor model is normally derived in Cartesian coordinate system [3]. In this paper analytical solution for magnetic field distribution in the Polar coordinate system will be used. Normally this coordinate system is used in designing process of rotational permanent magnet motors. With the appropriate approach and some simplifications the magnetic field distribution in the air-gap of linear PM motors can be calculated with this approach as well. In the rotational machines analytical derivation of mathematical model can be conducted for parallel or radial magnetization of permanent magnets. In our case, the solution for radial permanent magnet magnetization will be derived and used for magnetic field calculation of the magnetic field distribution in the air-gap of PM slotless linear motor model.

In the air-gap of permanent magnet synchronous motor the magnetic field can be calculated in two different regions presented in Fig. 3:
- in the air-space region (region I in Fig. 3);
- in the permanent magnets region (region II in Fig. 3).

The derivation of explicit solution for magnetic field calculation will be presented only for air-space region. Relation between magnetic field density vector $\mathbf{B}$ and magnetic field intensity vector $\mathbf{H}$ in the air-space is as following:

(1) $\mathbf{B}_{\mathrm{I}} = \mu_0 \mathbf{H}_{\mathrm{I}}$

and in the permanent magnets:

(2) $\mathbf{B}_{\mathrm{II}} = \mu_0 \mu_{\mathrm{r}} \mathbf{H}_{\mathrm{I}} + \mu_0 \mathbf{M}$

where $\mathbf{M}$ represents the residual magnetization vector and μ_{r} the relative recoil permeability. For permanent magnets with linear demagnetization characteristics (PM characteristic in the second-quadrant) the magnetization can be defined by (3):

(3) $$\mathbf{M} = \frac{\mathbf{B}_{\mathrm{r}}}{\mu_0}$$

where $\mathbf{B}_{\mathrm{r}}$ represents the remanence vector. For the magnetostatic field in the region without current densities the (4) and (5) can be written:

(4) $\mathrm{div}\mathbf{B} = \nabla \mathbf{B} = 0$

(5) $\mathrm{rot}\,\mathbf{B} = \nabla \times \mathbf{B} = 0$

The magnetic flux density $\mathbf{B}$ has a zero curl and it can be expressed as a gradient of a scalar field:

(6) $\mathbf{B} = -\mu_0 \mu_{\mathrm{r}} \nabla \varphi$

where φ denotes magnetic scalar potential.

By inserting (6) into the (4) the (7) can be obtained:

(7) $\nabla\left(-\mu_0 \mu_{\mathrm{r}} \nabla \varphi_{\mathrm{I}}\right) = 0 \;\Rightarrow\; \nabla\nabla\varphi_{\mathrm{I}} = \Delta\varphi_{\mathrm{I}} = 0$

In Polar coordinate system the magnetization vector $\mathbf{M}$ is given by:

(8) $\mathbf{M} = M_{\mathrm{r}} \overline{a_{\mathrm{r}}} + M_{\theta} \overline{a_{\theta}}$

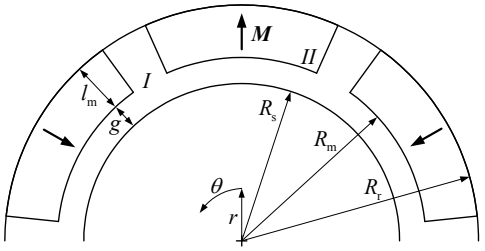

Fig. 3. Rotational PMSM with external rotor.

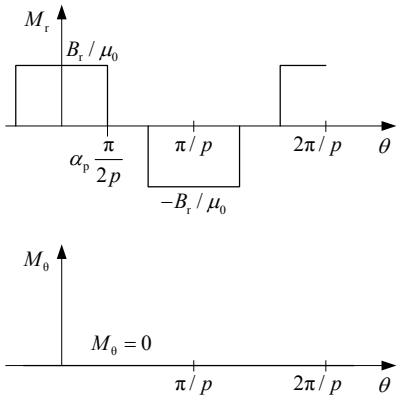

Fig. 4. Waveforms of magnetization vector components M_{r} and

The direction of magnetization vector $\mathbf{M}$ is depending on the type of magnetization of permanent magnets. In the case of radially magnetized magnets the vector $\mathbf{M}$ is perpendicular on the surface of the magnet and only radial component M_{r} exists, while the tangential component M_{θ} is equal zero. The waveform of radial in tangential component of magnetization vector $\mathbf{M}$ is presented in Fig. 4.

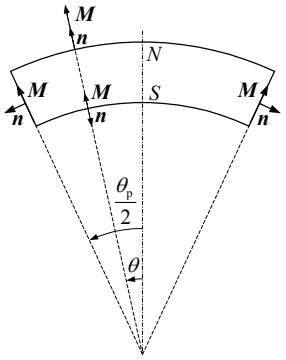

Fig. 5. Magnetization direction for radially magnetized magnets.

The presented radial and tangential components of magnetization vector can be written by Fourier series as:

(9) $$M_{\mathrm{r}} = \sum_{\mathrm{n}=1,3,5\ldots}^{\infty} M_{\mathrm{rn}} \cos(np\theta); \quad M_{\theta} = \sum_{\mathrm{n}=1,3,5\ldots}^{\infty} M_{\theta \mathrm{n}} \sin(np\theta)$$

where p is the number of pole pairs, θ is the angle between the centre of the magnet and the observation point (Fig. 5) and n is the number of used harmonics. For radially magnetized magnets the magnetization is:

(10) $$M_{\mathrm{rn}} = \frac{B_{\mathrm{r}}}{\mu_0} \frac{4}{n\pi} \sin\frac{n\pi\alpha_{\mathrm{p}}}{2}; \quad M_{\theta \mathrm{n}} = 0$$

where α_{p} is the ratio between the magnet pole arc and pole pitch.

Distribution of magnetic scalar potential in the air-space is given by the solution of Laplace's equation:

(11) $$\frac{\partial^2 \varphi_{\mathrm{I}}}{\partial r^2} + \frac{1}{r}\frac{\partial \varphi_{\mathrm{I}}}{\partial r} + \frac{1}{r^2}\frac{\partial^2 \varphi_{\mathrm{I}}}{\partial \theta^2} = 0$$

Relation between the magnetic field intensity vector $\mathbf{H}$ and magnetic scalar potential can be expressed as:

(12) $$\mathbf{H} = -\nabla\varphi = -\frac{\partial \varphi}{\partial r}\overrightarrow{a_{\mathrm{r}}} - \frac{1}{r}\frac{\partial \varphi}{\partial \theta}\overrightarrow{a_{\theta}}$$

where the radial H_{r} and tangential H_{θ} part of magnetic field intensity is:

(13) $$H_{\mathrm{r}} = -\frac{\partial \varphi}{\partial r}; \; H_{\theta} = -\frac{1}{r}\frac{\partial \varphi}{\partial \theta}$$

Determination of magnetic scalar potential distribution in air-space is a Laplacian two dimensional problem and can be solved out by the separation of variables. Scalar magnetic potential can be defined as product of two functions:

(14) $\varphi_{\mathrm{I}}(r,\theta) = R(r)F(\theta)$

Substituting (14) into (11) and dividing with RF/r^2 the equations (15) is obtained:

(15) $$\frac{r^2}{R}\frac{d^2R}{dr^2} + \frac{r}{R}\frac{dR}{dr} = -\frac{1}{F}\frac{d^2F}{d\theta^2} = \lambda^2$$

where λ is the separation constant. Both separated equations can be written as:

(16) $F'' + \lambda^2 F = 0$

(17) $r^2R'' + rR' - \lambda^2 R = 0$

The solution of second order differential equation (16) is in the form:

(18) $F(\theta) = C_1 \cos(\lambda\theta) + C_2 \sin(\lambda\theta)$

Distribution of magnetization is periodic even mathematical function (Fig. 4). Consequently the $F(\theta)$ is also periodic even function, which means that C_2 is equal zero and $\lambda = np$, equation (18) can be therefore rewritten as:

(19) $F(\theta) = C_1 \cos(\lambda\theta)$

Equation (17) is well known Cauchy-Euler equation and the solution of equation can be found in the form of $r = x^{\mathrm{k}}$. Solution of differential equation (17) can be written in the following form:

(20) $R(r) = C_3 r^{\mathrm{np}} + C_4 r^{-\mathrm{np}}$, n=1,2,3,…

Considering expression (19) and expression (20) in equation (14), the following solution is obtained:

(21) $\varphi_{\mathrm{nI}}(r,\theta) = (A_{\mathrm{nI}} r^{\mathrm{np}} + B_{\mathrm{nI}} r^{-\mathrm{np}})\cos(np\theta)$

where A_{nI} and B_{nI} are unknown constants which must be determined. With superposition method it is possible to determine a solution of φ_{nI} for different value of n. Sum of all particular solutions represent solution of (11). Therefore the solution for $\varphi_{\mathrm{I}}(r,\theta)$ is possible to be written by the following infinite series as:

(22) $$\varphi_{\mathrm{I}}(r,\theta) = \sum_{\mathrm{n}=1}^{\infty} (A_{\mathrm{nI}} r^{\mathrm{np}} + B_{\mathrm{nI}} r^{-\mathrm{np}})\cos(np\theta)$$

The boundary conditions from Fig. 3 are:

(23)
$$H_{\theta\mathrm{I}}(r,\theta)\big|_{\mathrm{r=Rs}} = 0$$
$$H_{\theta\mathrm{II}}(r,\theta)\big|_{\mathrm{r=Rr}} = 0$$
$$B_{\mathrm{rI}}(r,\theta)\big|_{\mathrm{r=Rm}} = B_{\mathrm{rII}}(r,\theta)\big|_{\mathrm{r=Rm}}$$
$$H_{\theta\mathrm{I}}(r,\theta)\big|_{\mathrm{r=Rm}} = H_{\theta\mathrm{II}}(r,\theta)\big|_{\mathrm{r=Rm}}$$

For a motor with external rotor the next two equations must be considered. First one is $R_{\mathrm{m}} = R_{\mathrm{s}} + g$ and the second one is $R_{\mathrm{r}} = R_{\mathrm{s}} + g + l_{\mathrm{m}}$, where R_{s} is the stator radius, R_{r} is the rotor radius, R_{m} is the magnet surface radius, g is the air-gap thickness and l_{m} is the radial thickness of permanent magnet. Complete solution for magnetic field density in the air-gap ($np \neq 1$) for radial component is as following:

(24)
$$B_{\mathrm{rI}}(r,\theta) = \sum_{\mathrm{n}=1,3,5\ldots}^{\infty} -\frac{\mu_0 M_{\mathrm{n}}}{\mu_{\mathrm{r}}} \frac{np}{(np)^2 - 1}\left[\left(\frac{r}{R_{\mathrm{m}}}\right)^{\mathrm{np-1}} + \left(\frac{R_{\mathrm{s}}}{R_{\mathrm{m}}}\right)^{\mathrm{np-1}}\left(\frac{R_{\mathrm{s}}}{r}\right)^{\mathrm{np+1}}\right]$$
$$\left\{\frac{(np-1)\left(\frac{R_{\mathrm{m}}}{R_{\mathrm{r}}}\right)^{2\mathrm{np}} + 2\left(\frac{R_{\mathrm{m}}}{R_{\mathrm{r}}}\right)^{\mathrm{np-1}} - (np+1)}{\frac{\mu_{\mathrm{r}}+1}{\mu_{\mathrm{r}}}\left[1 - \left(\frac{R_{\mathrm{s}}}{R_{\mathrm{r}}}\right)^{2\mathrm{np}}\right] - \frac{\mu_{\mathrm{r}}-1}{\mu_{\mathrm{r}}}\left[\left(\frac{R_{\mathrm{s}}}{R_{\mathrm{m}}}\right)^{2\mathrm{np}} - \left(\frac{R_{\mathrm{m}}}{R_{\mathrm{r}}}\right)^{2\mathrm{np}}\right]}\right\}\cos(np\theta)$$

And for the tangential component:

(25)
$$B_{\theta\mathrm{I}}(r,\theta) = \sum_{\mathrm{n}=1,3,5\ldots}^{\infty} -\frac{\mu_0 M_{\mathrm{n}}}{\mu_{\mathrm{r}}} \frac{np}{(np)^2 - 1}\left[\left(-\frac{r}{R_{\mathrm{m}}}\right)^{\mathrm{np-1}} + \left(\frac{R_{\mathrm{s}}}{R_{\mathrm{m}}}\right)^{\mathrm{np-1}}\left(\frac{R_{\mathrm{s}}}{r}\right)^{\mathrm{np+1}}\right]$$
$$\left\{\frac{(np-1)\left(\frac{R_{\mathrm{m}}}{R_{\mathrm{r}}}\right)^{2\mathrm{np}} + 2\left(\frac{R_{\mathrm{m}}}{R_{\mathrm{r}}}\right)^{\mathrm{np-1}} - (np+1)}{\frac{\mu_{\mathrm{r}}+1}{\mu_{\mathrm{r}}}\left[1 - \left(\frac{R_{\mathrm{s}}}{R_{\mathrm{r}}}\right)^{2\mathrm{np}}\right] - \frac{\mu_{\mathrm{r}}-1}{\mu_{\mathrm{r}}}\left[\left(\frac{R_{\mathrm{s}}}{R_{\mathrm{m}}}\right)^{2\mathrm{np}} - \left(\frac{R_{\mathrm{m}}}{R_{\mathrm{r}}}\right)^{2\mathrm{np}}\right]}\right\}\sin(np\theta)$$

With the equation (24) and the equation (25) the magnetic field density distribution in the air-gap of linear permanent magnet synchronous motor can be calculated. For adequate calculation the number of poles must be increased simultaneously with the increase of the rotor radius R_{r} at the same (preserved) dimensions of permanent magnets. In Fig. 6 the normal (radial) and tangential components of magnetic flux density in the air-gap are presented for different number of poles: $2p = 4$, $2p = 40$ and $2p = 400$. Difference between results of magnetic flux density distribution in the air-gap is negligible for $2p = 40$ and $2p = 400$. Calculated distribution of magnetic flux density is influenced by the number of considered harmonics n as well. Influence of considered number of harmonics on distribution of flux density is presented in Fig. 7 for following number of harmonics: $n = 4$, $n = 40$ and $n = 400$. Difference between calculated results of magnetic flux density is negligible for $n = 40$ and $n = 400$. The magnetic flux density in linear motor air-gap is also dependent on the distance from the surface of permanent magnets r. In Fig. 8 results for three different distances from the magnet surface are presented: $r = 0{,}5$ mm, $r = 2$ mm and $r = 4{,}5$ mm.

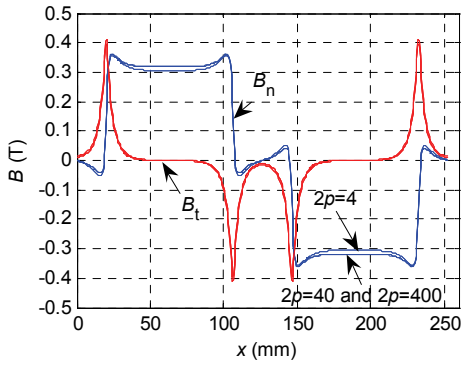

Fig. 6. Normal and tangential component for different number of poles, number of harmonics n=400 and distance from surface of magnets r =0,5 mm).

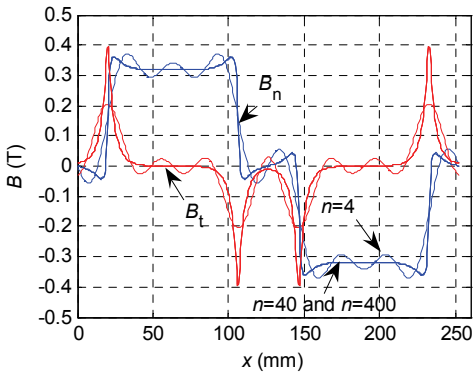

Fig. 7. Normal and tangential component for different number of harmonics, number of poles 2p =400 and distance from surface of magnets r =0,5 mm).

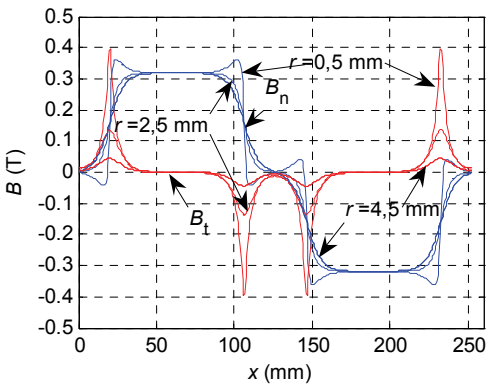

Fig. 8. Normal and tangential component for different distance from surface of magnets, number of poles 2p =400 and number of harmonics n=400.

Numerical calculation of magnetic field

Magnetic field density in linear permanent magnet motor model is numerically calculated with software package Ansys which is based on the well known finite element method. The mesh of aforementioned linear motor is shown in Fig. 9. Numerically calculated results of normal and tangential magnetic field density components are presented in Fig. 10.

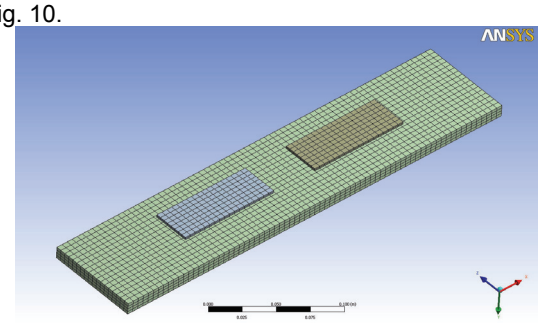

Fig. 9: Finite element mesh of linear permanent magnet motor model.

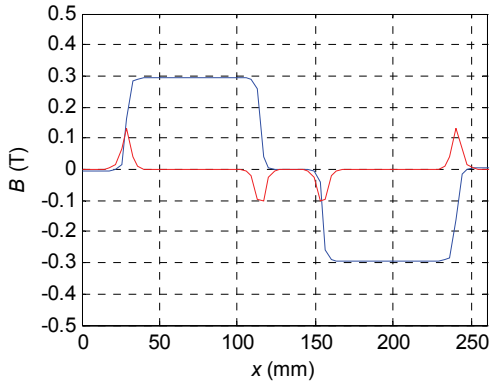

Fig. 10. Normal and tangential component of magnetic field density (distance from surface of magnets *r* =2,5 mm).

Experimetal setup for measurement of magnetic field

For confirmation of analytically and numerically calculated results the experimental setup was developed (Fig. 11). The experimental setup consists of two stepper motors which are controlled via personal computer by LabView software package. The magnetic field density is measured by Hall sensor. Both motors are used in positioning drive which carries the aforementioned Hall sensor (HS-TGB5-104005) and can be positioned in two directions with the resolution of 600 dpi in x-direction and 60 dpi in y-direction. The measured signal from sensor is leaded on Magnet-Physik FH54 measurement amplifier, measured with data acquisition card (National Instruments PCI 6251) and by PCI bus transferred to the personal computer. The three dimensional presentation of measured results of normal and tangential magnetic field density components are presented in Fig. 12 and Fig. 13.

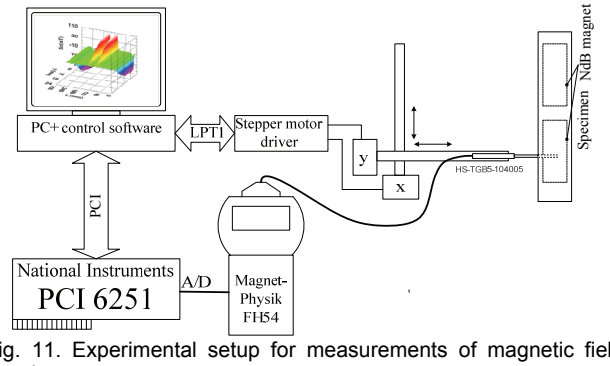

Fig. 11. Experimental setup for measurements of magnetic field density.

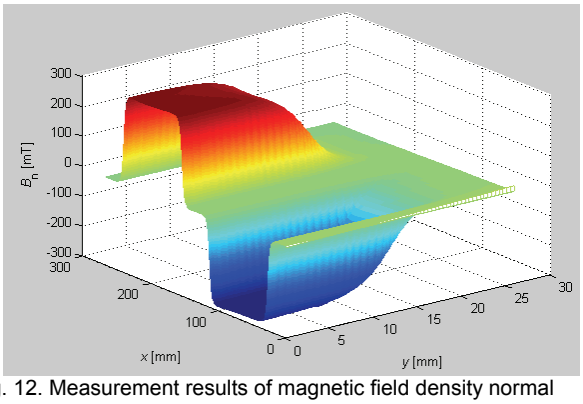

Fig. 12. Measurement results of magnetic field density normal component (distance from surface of magnets *r* =2,5 mm).

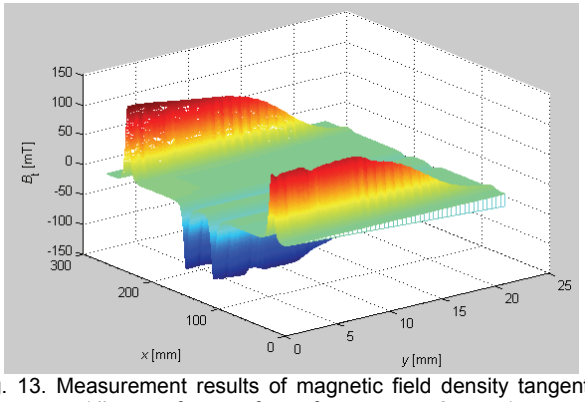

Fig. 13. Measurement results of magnetic field density tangential component (distance from surface of magnets *r* =2,5 mm).

Comparison of results

In order to confirm the analytically and the numerically calculated results in this research the comparison with measured results is a necessity. In Fig. 14 and Fig. 15 the comparison of calculated and measured results is presented. Analytically calculated results are presented with the black colour, numerically calculated results are presented with the blue colour and measured results with the red colour.

Fig. 14 presents the results of the normal component of the magnetic field density, calculated and measured in distance 2,5 mm from the surface of permanent magnets. The calculated peak values of magnetic field density waveform are almost the same, when compared to the measured peak value. The reason for deviation is the magnet's remanence which in real permanent magnets can deviate from the nominal value.

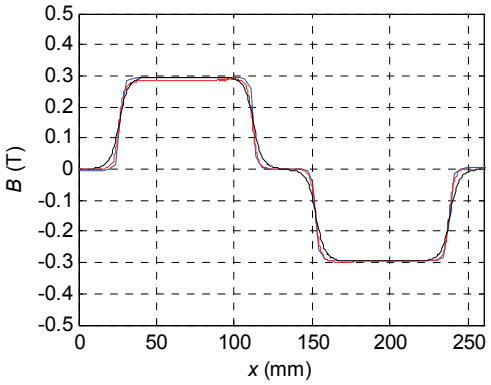

Fig. 14. Comparison of calculated and measured results of magnetic field density normal component (distance from surface of magnets *r* =2,5 mm).

Fig. 15 presents the results of the tangential component of the magnetic field density, calculated and measured in

distance 2,5 mm from the surface of permanent magnets. The calculated results of magnetic field density agree very well with the measured ones.

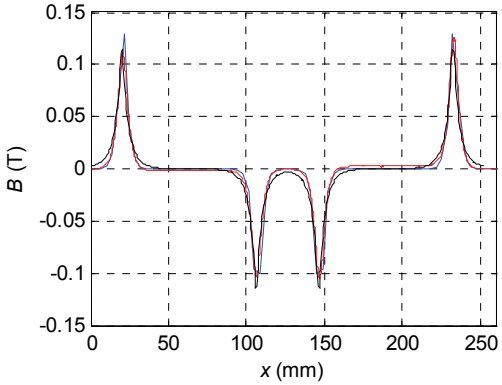

Fig. 15. Comparison of calculated and measured results of magnetic field density tangential component (distance from surface of magnets r =2,5 mm).

Conclusion

For a detailed and precise analysis of magnetic field in the linear permanent magnet motor model, three different approaches for determination of magnetic filed density were employed. The paper presented the mathematical derivation for the analytical calculation of normal and tangential magnetic flux density components in Polar coordinate system. Numerical calculations were performed by the finite element method. For confirmation of the calculated results, the experimental setup for measuring magnetic flux densities was developed. The comparison of the calculated and measured results was presented as well. These show good agreement between calculated and measured results. The results of this research are practically useful in the design of permanent magnet electrical machines.

REFERENCES

[1] Virtič P., Štumberger B., 2D Analytical Solution of Magnetic Field in Linear Permanent Magnet Synchronous Machine; Comparison of Analytical and Numerical Solution of Magnetic Field by Permanent Magnets, Prz. Elektrotech., Vol. 83, No. 7-8, p.p. 139-142.

[2] Zhu Z. Q., Howe D., Analytical Prediction of the Cogging Torque in Radial-Field Permanent-Magnet Brushless Motors, IEEE Transactions on Magnetics, Vol. 28, No. 2, p.p. 1371-1374, March 1992.

[3] Zhu Z. Q., Howe D., Bolte E., et al., Instantaneous Magnetic-Field Distribution in Brushless Permanent-Magnet DC Motors: I. Open-Circuit Field, IEEE Transactions on Magnetics, Vol. 29, No. 1, p.p. 124-135, Januar 1993.

[4] Azzouzi J., Barakat G., Dakyo B., Quasi-3-D Analytical Modeling of the Magnetic Field of an Axial Flux Permanent-Magnet Synchronous Machine, IEEE Transactions on Energy Conversion, Vol. 20, No. 4 p.p. 746-752, December 2005.

[5] Virtič P., Hadžiselimović M., Štumberger B., Static Thrust and Normal Force Calculation in a Slotless-Type Permanent Magnet Linear Synchronous Motor. Prz. Elektrotech., Vol. 83, No. 12, p.p. 118-121, 2007.

***Authors**: Miralem Hadžiselimović, Peter Virtič, Bojan Štumberger University of Maribor, Faculty of Energy Technology, Hočevarjev trg 1, 8270 Krško, Slovenia, E-mail: miralem.h@uni-mb.si; Viktor Goričan, University of Maribor, Faculty of Electrical Engineering and Computer Science, Smetanova 17, 2000 Maribor, Slovenia; Tine Marčič, TECES, Development Centre for Electrical Machines, Pobreška cesta 20, 2000 Maribor, Slovenia.*